NASA TM X-673

NASA TM X-673

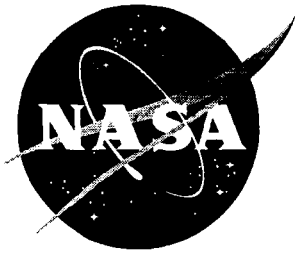

TECHNICAL MEMORANDUM

X-673

TRANSONIC DYNAMIC LONGITUDINAL STABILITY CHARACTERISTICS OF SIX BALLISTIC REENTRY CONFIGURATIONS DESIGNED FOR SUPERSONIC IMPACT

By Ernest R. Hillje and Robert A. Kilgore

Langley Research Center

NATIONAL AERONAUTICS AND SPACE ADMINISTRATION

WASHINGTON

March 1962

NATIONAL AERONAUTICS AND SPACE ADMINISTRATION

TECHNICAL MEMORANDUM X-673

TRANSONIC DYNAMIC LONGITUDINAL STABILITY CHARACTERISTICS OF SIX BALLISTIC REENTRY CONFIGURATIONS DESIGNED FOR SUPERSONIC IMPACT*

By Ernest R. Hillje and Robert A. Kilgore

SUMMARY

An investigation has been made in the Langley 8-foot transonic pressure tunnel to determine the damping-in-pitch and the oscillatory longitudinal stability characteristics of six blunt-nose cylinder-flare reentry configurations that were designed for supersonic impact. Tests were made at Mach numbers from 0.80 to 1.15 and at mean angles of attack from 0° to 14°. Reynolds numbers, based on 0.333 foot, varied from 0.62×10^6 to 0.69×10^6. The amplitude of the forced oscillation was 2° with reduced frequencies from 0.012 to 0.036. Some of the effects of flare angle, nose shape, and fins are noted.

INTRODUCTION

The Langley Research Center is conducting a research program to determine the static and dynamic stability characteristics of several ballistic reentry configurations designed for supersonic impact. Since, for certain short or intermediate range missions, a particular reentry configuration might be subjected to transonic or high subsonic speeds before impact, it was considered necessary to determine the stability characteristics of the several shapes at transonic speeds.

The static stability characteristics for several of the configurations at transonic speeds are presented in reference 1 and for supersonic speeds in references 2, 3, and 4. The dynamic stability characteristics at supersonic speeds are presented in references 5, 6, and 7.

Presented herein are the results of tests to determine the damping-in-pitch and the oscillatory longitudinal stability characteristics of

*Title, Unclassified.

six reentry configurations at Mach numbers from 0.80 to 1.15 and at mean angles of attack from 0° to 14°.

SYMBOLS

All aerodynamic data in this report are presented in the body system of axes with moments referred to the model oscillation axis as shown in figure 1.

A	reference area, $\pi d^2/4$, 0.0871 sq ft
C_m	pitching-moment coefficient, $\frac{\text{Pitching moment}}{\rho\frac{V^2}{2} Ad}$
d	reference length, model diameter at nose-body juncture, 0.333 ft
M	free-stream Mach number
q	angular velocity in pitch, radians/sec
R	Reynolds number based on d
V	free-stream velocity, ft/sec
α	instantaneous angle of attack, radians
α_m	mean angle of attack, deg
ρ	free-stream mass density, $\frac{\text{lb-sec}^2}{\text{ft}^4}$
ω	2π(Frequency of oscillation), radians/sec
$\frac{\omega d}{V}$	reduced-frequency parameter, radians

$C_{m_\alpha} = \frac{\partial C_m}{\partial \alpha}$, per radian

$$C_{m_{\dot{\alpha}}} = \frac{\partial C_m}{\partial\left(\frac{\dot{\alpha} d}{V}\right)}, \text{ per radian}$$

$$C_{m_q} = \frac{\partial C_m}{\partial\left(\frac{q d}{V}\right)}, \text{ per radian}$$

$$C_{m_{\dot{q}}} = \frac{\partial C_m}{\partial\left(\frac{\dot{q} d^2}{V^2}\right)}, \text{ per radian}$$

$C_{m_\alpha} - \left(\frac{\omega d}{V}\right)^2 C_{m_{\dot{q}}}$ oscillatory longitudinal stability parameter, per radian

$C_{m_q} + C_{m_{\dot{\alpha}}}$ damping-in-pitch parameter, per radian

A dot above a symbol denotes a derivative with respect to time.

MODELS AND APPARATUS

Sketches of the six models used for the investigation are shown in figure 1. Configurations 1, 2, and 3 have the same short, truncated-cone nose geometry but differ in flare angle and flare length. Configurations 3, 4, and 5 have the same afterbody shapes but differ in nose shape. The six flared fins of configuration 6 are symmetrically disposed about a cylindrical afterbody; this configuration has the same maximum projected plan area as that of configuration 1. All the models were oscillated about a point 11.12 inches forward of the base with the exception of the model of configuration 5, for which the oscillation axis was 10.62 inches forward of the base.

The models were machined from steel, except for the fins of the model of configuration 6 which were constructed of plastic. All models were tested in the aerodynamically smooth condition except for the round-nose model (configuration 5) which had a 0.12-inch-wide strip of 0.011-inch nominal-diameter carborundum grains at the intersection of the spherical and conical sections of the nose, as can be seen in figure 1. Calculations based on the method presented in reference 8 indicate that roughness of this size should be sufficient to cause transition from a laminar to a turbulent boundary layer. Each model had a

flat base with an opening of approximately 3 inches in diameter to accommodate the supporting sting.

The models were mounted on a strain-gage balance which was rigidly forced to perform a pitching oscillation. The oscillation-balance mechanism used for these tests is described in detail in reference 9. The tests were conducted in the Langley 8-foot transonic pressure tunnel.

TESTS

Tests were conducted at Mach numbers from 0.80 to 1.15 and at mean angles of attack from 0° to 14°. Reynolds numbers, based on a reference diameter d of 0.333 foot, varied from 0.62×10^6 to 0.69×10^6. No data were taken for Mach numbers at which wall-reflected shock disturbances would intersect the model. Tunnel stagnation temperature was automatically held at 122° F and humidity was maintained at a level such that the air flow was free of condensation shocks.

Aerodynamic data were measured at frequencies near the natural frequency of the oscillating model system to insure the most accurate determination of the damping parameter. (See ref. 10.) The amplitude of oscillation was 2° and the reduced-frequency parameter $\omega d/V$ varied from 0.012 to 0.036.

RESULTS AND DISCUSSION

Effects of Flare Angle

For configurations 1, 2, and 3, which have the same nose geometry and flare-base diameter but have different longitudinal locations of the body-flare juncture (fig. 1), the oscillatory stability parameter $C_{m_\alpha} - \left(\frac{\omega d}{V}\right)^2 C_{m_{\dot{q}}}$ generally becomes more negative (indicating increasing positive stability) as the body-flare juncture is moved rearward. (See fig. 2.) This trend is in agreement with the static results of reference 1. Configuration 1, which has the smallest flare angle of 3.87°, is marginally stable or unstable for all test conditions and, as pointed out in reference 1, may be unsuitable aerodynamically for use as a ballistic reentry configuration. Negative values of the damping-in-pitch parameter $C_{m_q} + C_{m_{\dot{\alpha}}}$ (indicating positive damping) were measured for these three configurations. At the subsonic Mach numbers the level of damping increases with increased flare angle.

Effects of Nose Shape

The effects of nose shape on the dynamic longitudinal stability characteristics are presented in figure 3 for configurations 3, 4, and 5, all of which have the same body-flare combination. The negative values of the oscillatory stability parameter $C_{m_\alpha} - \left(\frac{\omega d}{V}\right)^2 C_{m_q}$ show all three configurations to be stable. The large increase in stability at $M = 0.90$ and $\alpha_m = 0^\circ$ for configuration 5, the model with the round nose, was also obtained in the static investigation of reference 1.

All three configurations had positive pitch damping at all test conditions with one notable exception. For configuration 5, there appears a negative damping peak at $M = 1.00$ and $\alpha_m = 8^\circ$; this negative value indicates an energy input to the model system. At this condition, the measurements were not very repeatable, as can be seen by the spread in the data. References 11 and 12 and unpublished data at the Langley Research Center for some similar flare-stabilized bodies show negative damping peaks for test conditions where a sharp break occurs in the variation of pitching moment with angle of attack. The negative damping is attributed to the fact that the oscillating model is subjected to alternately attached and separated flow during each cycle of oscillation. Although the stability parameter $C_{m_\alpha} - \left(\frac{\omega d}{V}\right)^2 C_{m_q}$ of the present tests does not define a sharp break at the test conditions where the negative damping peak occurs, the static stability data of reference 1 do show nonlinearities for this round-nose configuration at these test conditions; these nonlinearities indicate a region of changing flow conditions. The data of reference 1 also show nonlinearities at $M = 0.95$ near $\alpha = 4^\circ$ and at $M = 0.90$ near $\alpha = 2^\circ$. Had dynamic stability tests of the present investigation included these ranges of angle of attack and Mach number, it is probable that negative damping peaks would also have been measured at these test conditions.

Effect of Fins

In figure 4, comparison of the data for configuration 6, which has six fins flared 3.87°, with the data for configuration 1, which has a conical flare of 3.87°, shows greater stability for the finned configuration, particularly at the high angles of attack. As previously mentioned in the section "Models and Apparatus," these two configurations have the same projected plan area. The pronounced differences in the stability parameters contrast sharply with the similarities in the damping parameters.

SUMMARY OF RESULTS

The transonic longitudinal damping and oscillatory stability of six blunt-nose cylinder-flare reentry configurations have been determined and the principal results are summarized as follows:

1. All configurations showed positive damping except for the round-nose configuration at a Mach number of 1.00 and at a mean angle of attack of 8° where a negative damping peak occurred.

2. Except for the configuration with a flare angle of 3.87°, all configurations had positive oscillatory stability.

3. For the configurations with the short truncated-cone nose, the oscillatory stability increased at all Mach numbers and the damping increased at the subsonic Mach numbers with increasing flare angle.

4. The round-nose configuration with the 10° flare had about twice the oscillatory stability at a Mach number of 0.90 and at mean angle of attack of 0° as did the body-flare configurations with the truncated-cone noses.

5. The configuration with fins flared 3.87° had greater stability than the configuration with conical flare of 3.87°, particularly at the high angles of attack. Both configurations had the same level of damping.

Langley Research Center,
National Aeronautics and Space Administration,
Langley Air Force Base, Va., January 25, 1962.

REFERENCES

1. Mugler, John P., Jr.: Transonic Wind-Tunnel Investigation of the Static Longitudinal Aerodynamic Characteristics of Five Nose Cones Designed for Supersonic Impact. NASA TM X-432, 1961.

2. Gregory, Donald T., and Carraway, Ausley B.: An Investigation at Mach Numbers From 1.47 to 2.87 of Static Stability Characteristics of Nine Nose Cones Designed for Supersonic Impact Velocities. NASA TM X-69, 1959.

3. Swihart, John M.: Static Stability Investigation of Supersonic-Impact Ballistic Reentry Shapes at Mach Numbers of 2.55 and 3.05. NASA MEMO 5-27-59L, 1959.

4. Shaw, David S., and Reed, James D.: Wind-Tunnel Investigation at Mach Numbers From 1.47 to 4.62 of Static Aerodynamic Characteristics of Twelve Nose Cones Designed for Supersonic Impact. NASA TM X-545, 1961.

5. Fletcher, Herman S., and Wolhart, Walter D.: Damping in Pitch and Static Stability of Supersonic Impact Nose Cones, Short Blunt Subsonic Impact Nose Cones, and Manned Reentry Capsules at Mach Numbers From 1.93 to 3.05. NASA TM X-347, 1960.

6. Fletcher, Herman S.: The Damping in Pitch and Static Stability of Six Supersonic-Impact Ballistic Configurations and Three High-Drag Reentry Capsules at a Mach Number of 6.83. NASA TM X-349, 1961.

7. Fletcher, Herman S.: Damping in Pitch and Static Stability of Blunt Cone-Cylinder-Flare Models and Manned Reentry Capsule Models for Various Angles of Attack at a Mach Number of 2.91. NASA TM X-539, 1961.

8. Braslow, Albert L., and Knox, Eugene C.: Simplified Method for Determination of Critical Height of Distributed Roughness Particles for Boundary-Layer Transition at Mach Numbers From 0 to 5. NACA TN 4363, 1958.

9. Bielat, Ralph P., and Wiley, Harleth G.: Dynamic Longitudinal and Directional Stability Derivatives for a 45° Sweptback-Wing Airplane Model at Transonic Speeds. NASA TM X-39, 1959.

10. Braslow, Albert L., Wiley, Harleth G., and Lee, Cullen Q.: Dynamic Directional Stability Derivatives for a 45° Swept-Wing—Vertical-Tail Airplane Model at Transonic Speeds and Angles of Attack, With a Description of the Mechanism and Instrumentation Employed. NACA RM L58A28, 1958.

11. Reese, David E., Jr., and Wehrend, William R., Jr.: An Investigation of the Static and Dynamic Aerodynamic Characteristics of a Series of Blunt-Nosed Cylinder-Flare Models at Mach Numbers From 0.65 to 2.20. NASA TM X-110, 1960.

12. Tunnell, Phillips J., Marker, Ralph D., and Reese, David E., Jr.: Characteristics of a Blunt-Nosed Cylindrical Flared Body in Pitch at Transonic Mach Numbers. NASA TM X-159, 1960.

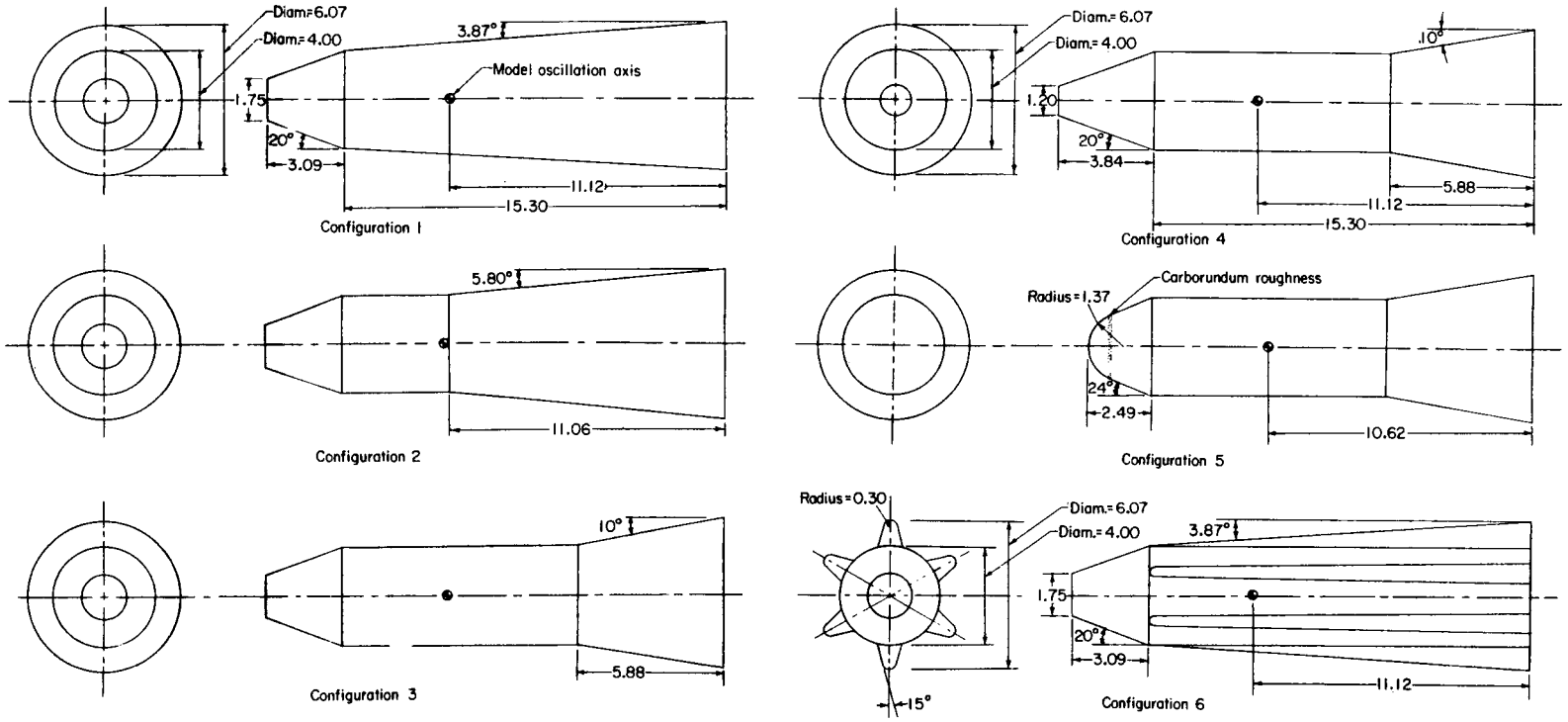

Figure 1.- Sketch of models. All linear dimensions are in inches.

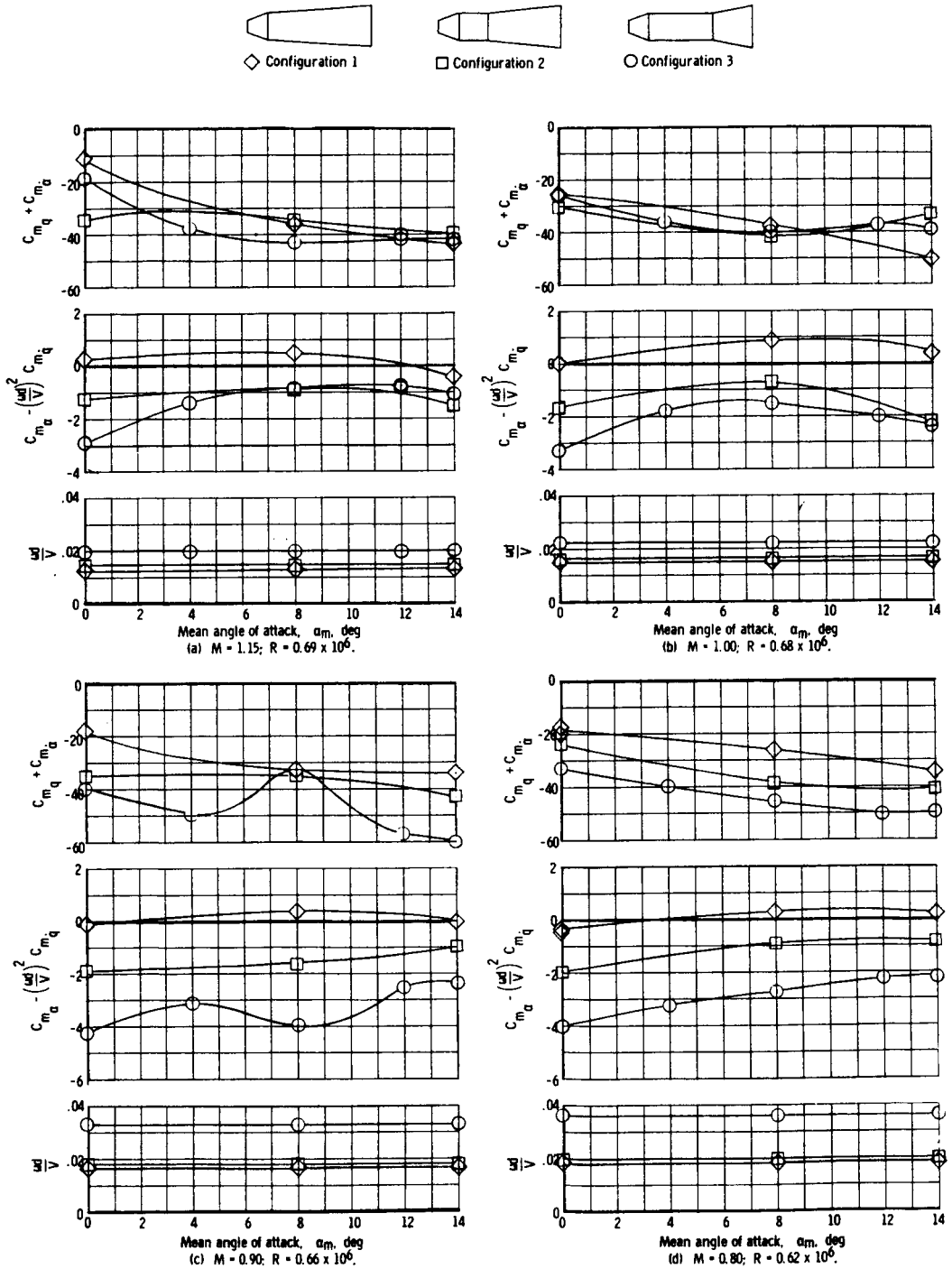

Figure 2.- Effect of change of flare angle and flare length on damping-in-pitch parameter and oscillatory longitudinal stability parameter for various Mach numbers.

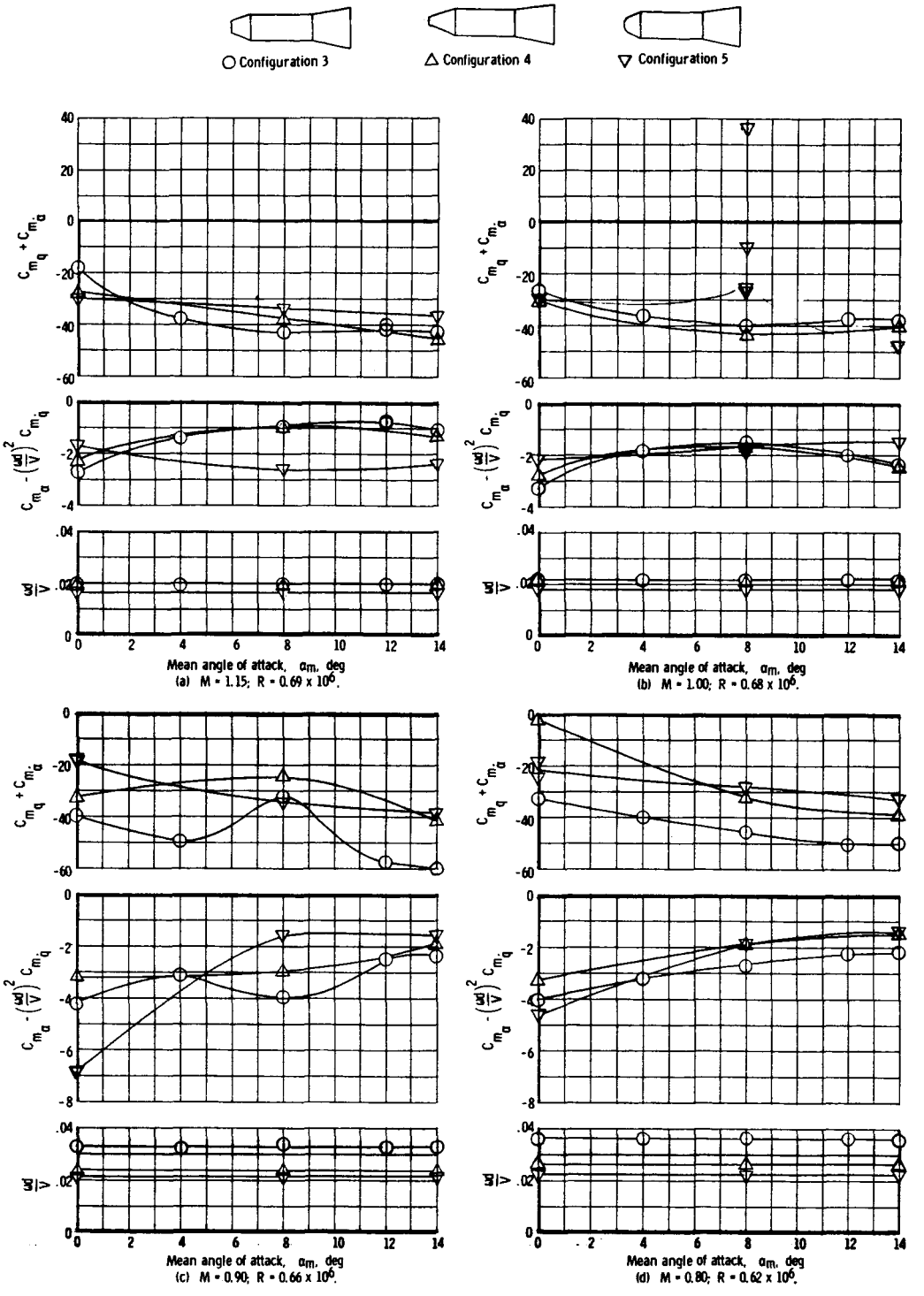

Figure 3.- Effect of nose shape on damping-in-pitch parameter and oscillatory longitudinal stability parameter for various Mach numbers.

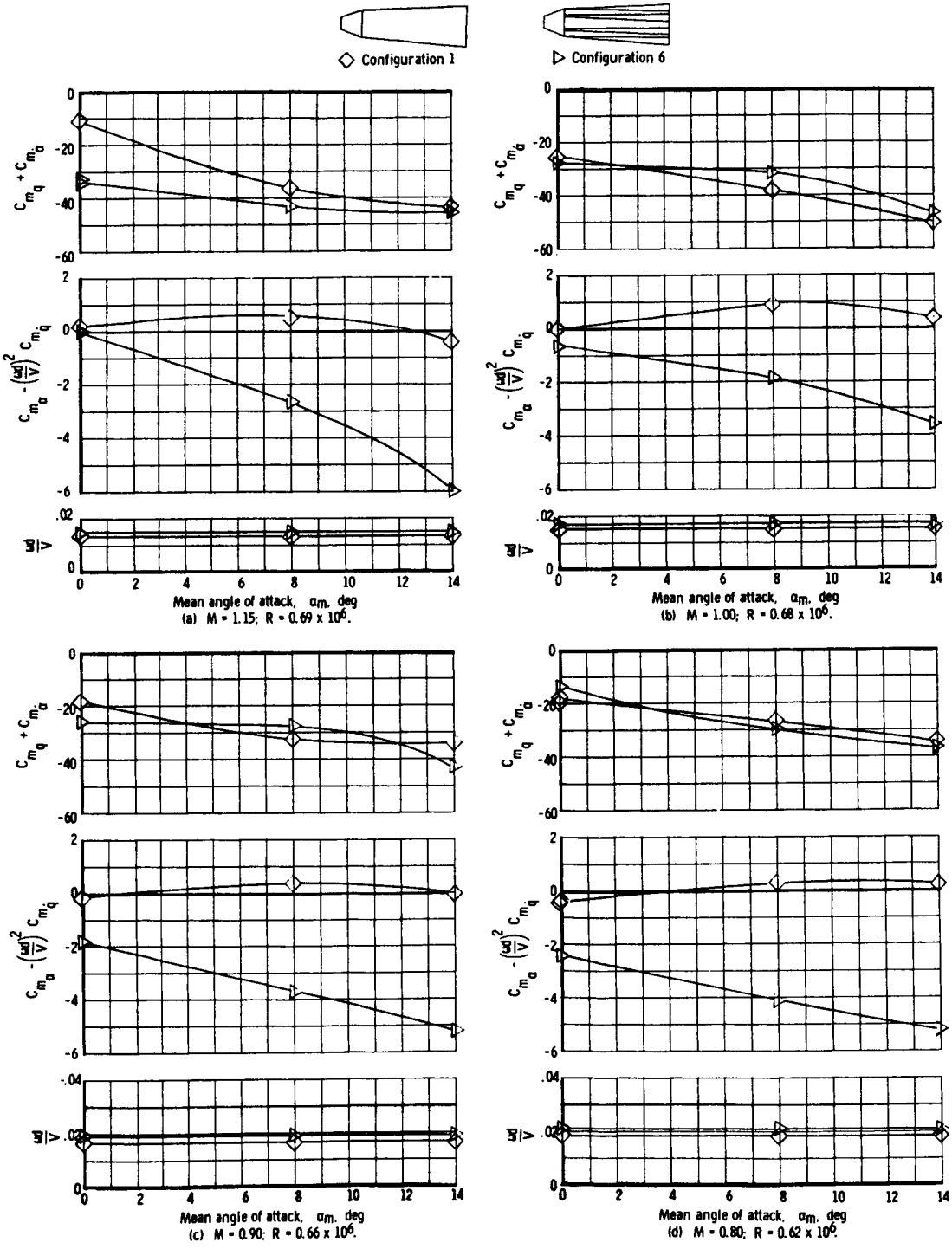

Figure 4.- Effect of fins on damping-in-pitch parameter and oscillatory longitudinal stability parameter for various Mach numbers.